

Weak-Antilocalization induced Enhanced Surface Conductivity and topological protection in Topological Insulator Thin films

R.K. Gopal, Sourabh Singh, Arpita Mandal, Jit Sarkar, Sandeep Tammu, Partha Mitra, Chiranjib Mitra

Indian Institute of Science Education & Research Kolkata, Mohanpur - 741246, India

Abstract:

We report magnetotransport measurements on ternary tetradymite Topological Insulating compound $\text{Bi}_2\text{Se}_2\text{Te}$ thin films deposited by pulsed laser deposition technique. The temperature dependent resistance of these thin films shows insulating ground state followed by insulator to surface metallic transition at low temperature. Hence we anticipate that the chemical potential of these thin films lie in the bulk insulating gap, a fundamental requirement of topological insulating materials for the device applications. Such a bulk insulating state is known as the topological transport regime as shown by temperature dependence of resistance. Manifestation of topological protection and surface dominated transport has been elaborately explained by weak antilocalization data and low temperature (less than 50K) down turn in resistance of these thin films. The Magnetoresistance of these thin films exhibit pronounced weak antilocalization behavior with a sharp cusp in the vicinity of zero magnetic field. Surface states have been found remarkably robust even at reasonably high temperatures (100K) exhibiting linear MR in high field regime in agreement with other reports. Our findings are crucial for the understanding of transport behavior of TI's and pave the way towards realizing novel device applications.

Introduction:

Presence of an odd number of helical Dirac cones on the surface and a π Berry phase have made Topological insulators (TI) a promising class of materials that exhibit numerous exotic phenomena such as topological delocalization towards time reversal invariant (non-magnetic) impurities and defects¹⁻⁴. The linear dispersion of these surface Dirac states along with helical spin texture make them distinct from other trivial two dimensional surface states (2DEG) or other strongly spin orbit coupled (SOC) systems. These spin filtered Dirac states are robust to any amount of non-magnetic disorder, interactions and defects which is in stark contrast to the trivial 2DEG systems and SOC systems, which become localized when subjected to the disorder. This nontrivial phase of insulators have been characterized by a Z_2 topological quantum number which makes this phase distinct from conventional insulators with bulk gap: $Z_2=-1$ and 0 for TI (2D, while four Z_2 invariants for the classification in 3D TIs)and trivial insulators respectively^{5,6,7}. This topological classification ensures that smooth deformations in the system

will not change the physical properties of the TI, but cannot be deformed in to a trivial insulator unless the gap closes. The topological order of the bulk wave function is responsible for such nontrivial states appearing on the surface of a TI as odd number of Dirac cones. This Z_2 topologically ordered state guarantees presence of odd number of Fermi surface owing to formation of Kramer's doublet and decides the number of surface modes (edge modes in 2D) which cannot be gapped by tuning the disorder (chemical potential). This type of even/odd topological effects is manifested in the magnetotransport, surface sensitive probes and magneto-optical experiments. It is this Z_2 quantum number which (even –odd number of Dirac cones) which separates TI's fundamentally from graphene.

There are a number of evidences on surface dominated transport on thin films and nano-devices, exhibiting two dimensional nature of quantum interference phenomena like two dimensional weak antilocalization(WAL), Shubnikov de – Hass (SdH) oscillations and Aharonov – Bohm(AB)Oscillations in magnetoresistance^{8–11,12,13}. These experiments provide direct evidence of quantum mechanical nature of these robust Dirac states exhibiting quantum interference while encountering an impurity on their way. Impurities and defects act like an obstacle or slit to ordinary waves^{14–16,17,18}. Their intensity pattern depends on the relative phase between the two paths, which is also true in case of Dirac states having shown unequivocally a Berry phase of π in MR oscillations mentioned above^{19,20,21,22}. The device application of TI's in terms of spintronics is not far away since some of remarkable applications are already underway on the basis of recent results²³.

In the past few years there has been an intense search for better topological insulators than the earlier binary alloys Bi_2Te_3 (BT), Bi_2Se_3 (BS) and Sb_2Te_3 (ST). That is because these alloys have finite residual bulk contribution to transport as is evident from transport experiments, which in turn masks the surface transport signals. These alloys are not in the so called topological transport regime. In topological transport regime the Fermi level lies in the bulk gap, thus making the bulk insulating and conduction is dominated by the surface electrons arising out of the Dirac like surface states^{24–34}. This has been well established by surface sensitive probes such as angle resolved photoemission experiments and scanning tunneling spectroscopy/microscopy on binary and ternary TI materials. Significant efforts have been devoted to suppress these defect induced bulk conduction which include compensation doping (Sn, Cd, Sb, etc.) and electrostatic tuning of the Fermi level. But still there are contributions from the metallic bulk and the doping further aggravates the situation by introducing structural defects. Therefore these extrinsic TI's do not seem to be promising candidates. Ternary and quaternary topological insulators materials, $\text{Bi}_2\text{Se}_2\text{Te}$ (BST), $\text{Bi}_2\text{Te}_2\text{Se}$ (BTS), $\text{Bi}_{2-x}\text{Sb}_x\text{Te}_3$, $\text{Bi}_{2-x}\text{Sb}_{1-x}\text{Se}_3$ and $\text{Bi}_x\text{Sb}_{1-x}\text{Te}_y\text{Se}_{1-y}$ (BSTS), on the other hand seem to be having the Fermi level inside the band gap^{32–35}. ARPES measurement validates the above point and hence these ternary tetradymites fulfill the criteria of intrinsic topological insulators. Thus these materials are ideal and promising candidates for realizing surface dominated transport leading to fabrication of spintronic devices harnessing surface Dirac electrons. BTS has been well established as a better topological insulator by means of several transport and spectroscopic studies performed on it (showing bulk resistivity as high as 6

ohm.cm at 4K), but less attention has been paid on BST which is considered to be a better candidate in terms of spin texture and lesser hexagonal warping of the Dirac cone²⁹.

In the case of BST the Dirac point is located nearly in the center of the band gap, while for BTS it is embedded downwards in the bulk valence band. This location of the Dirac point for BST and BTS is due to the derivation of these compounds from parent materials, BS and BT respectively. It is therefore interesting to note here that although BTS has high resistivity, but to observe various exotic phenomena such as topological magneto-electric effect by opening gap in the surface states, BST is much more promising owing to its unique positioning of the isolated Dirac point. Currently the focus has been shifted towards these materials in terms of compositional and band structure engineering owing to their superiority over binary alloys.

Moreover, it has been experimentally verified that the shape of the Dirac cone and position of the Dirac point changes with the proper compositional engineering. Previously Dirac dispersion in binary TI's was found to be little nonlinear away from the Dirac point^{32,36,37}. Tuning of these band structure parameters has profound effect on the surface electronic dominated transport and optical properties: Fermi velocity of Dirac states (slope of Dirac cone) increases and it is easy to manipulate surface states in the bulk gap (Ambipolar surface conduction)³². The transport signature of the surface Dirac states have been achieved unambiguously with very less or no parasitic bulk effects in such ternary and quaternary TI devices/single crystals. Recent spin sensitive experiments performed on these material devices have clearly demonstrated Dirac states dominated features up to remarkable high temperatures³⁸.

Another advantage of these ternary materials in comparison to binary ones is the presence of topological surface states below Dirac point with high degree of spin texture (reduced hexagonal warping), which was found to be buried in the bulk valence bands in the latter case. Therefore for the device storage and spintronics applications both Dirac cones could be accessed easily. These observations have been revealed in spin resolved photoemission experiments, justifying unambiguously the topological nature of surface states well below Dirac point²⁹. Moreover, their experimental observation clearly shows better Dirac cone structure in terms of hexagonal warping, spin polarizability and position of Dirac cone itself in the bulk gap. These properties of materials with high bulk insulating character have certainly paved the way for spintronics and other device applications.

Experimental:

BST thin films were grown on Si (001) substrates at different temperatures (250°C- 350°C). Substrate heating is an important parameter for epitaxial and ordered growth of thin films. The composition and quality of the film is affected by the reaction kinetics and the reaction rate of the reactant species. The substrate temperature controls both the reaction rate and its kinetics. We observed that samples prepared in 250°C – 300°C were better in comparison to the ones grown on high substrate temperature in terms of morphology, grain size and crystal structure³⁹⁻⁴¹. The substrates were cleaned by immersing them in 5% HF solution for 10 minutes followed by ultrasound bath for 15 minutes in DI water. Prior to growth substrates were degassed at elevated temperature of 400°C and subsequently flushed by inert gas (Argon) twice to get rid of

impurities and oxide contaminations on the surface. Substrates were then cooled slowly to the deposition temperature. The ablation target material for BST thin films was prepared by grinding BS and BT materials in a stoichiometric ratio of 2:1 to get exact BST composition of thin films. The finely ground resultant material was pressed to form a pellet and subsequently it was then annealed at 400°C for 4hr in an inert (Argon) atmosphere followed by cooling it slowly for 4hrs.

Thin films of thicknesses nearly 300nm to 500nm were deposited at low repetition rate of 1Hz and at a laser fluence of 1.5J/cm². All the results reported in this work are of 300nm thick sample. After deposition, the films were annealed in Argon environment for nearly two hours, cooling the films slowly to room temperature.

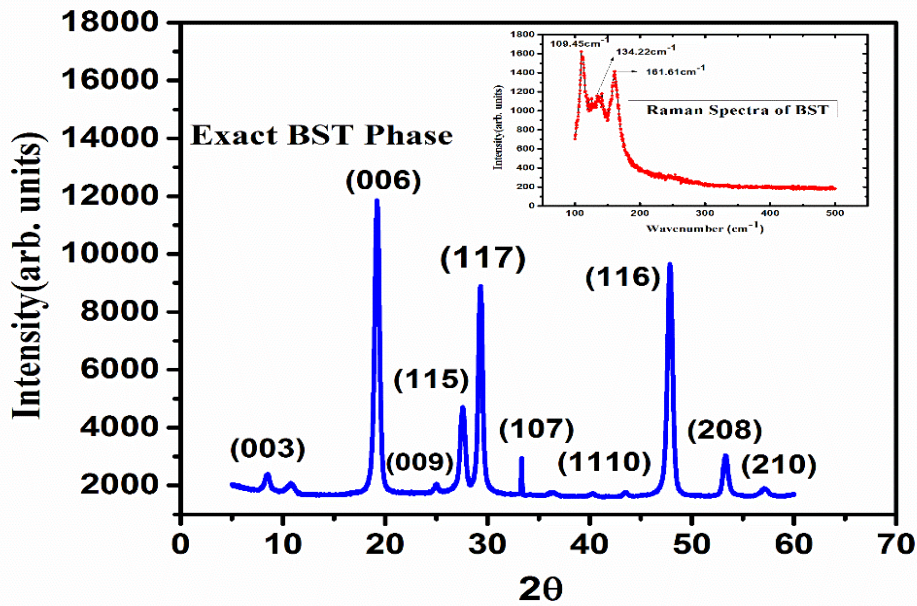


Fig. 1 XRD pattern of BST thin film. Raman spectrum is shown in the inset.

The BST thin films were characterized by X-ray diffraction and Raman spectroscopy as shown in Fig.1. From the XRD analysis it is clear that thin films are in ordered phase of BST and hence are crystalline in nature. Three characteristic Raman peaks have been identified at the position 109.45 cm⁻¹, 134.22 cm⁻¹ and 161.61 cm⁻¹. These peaks correspond to the doubly degenerate Raman modes E_{2g} and A_{1g}² respectively which are characteristic of the BST sample as previously reported.

Results and Discussion

Transport measurements on thin films were carried out in a cryogen free magnet (Cryogenic, U.K.) in the temperature range of 1.78K to 300K and a maximum magnetic field of 8 Tesla.

Before placing the sample inside the cryogenic system a Hall bar pattern was fabricated using optical lithography technique.

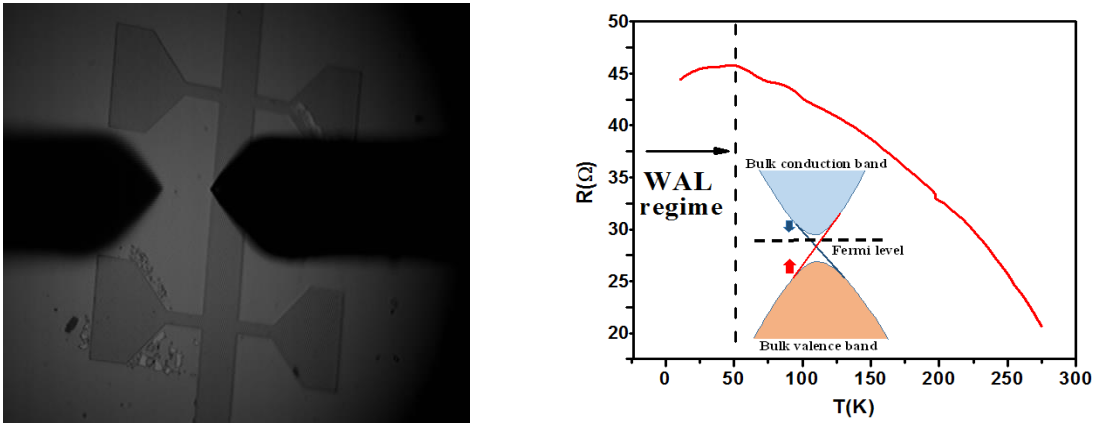


Fig. 2. **(a)** Hall bar pattern on the BST thin film sample. The black shadow depicts the arms of the profilometer used to measure the thickness of the sample. **(b)** Resistance variation with temperature. The figure clearly depicts the insulating behavior of BST thin films down to 50K and thereafter it shows insulator to metal transition due to onset of Weak Antilocalization (WAL) which dominates over other interactions, such as electron – phonon and electron - electron interactions. The dashed vertical line delineates WAL regime from bulk insulating regime.

As it can be seen from the Resistance vs. Temperature (R-T) plot in Fig. 2(b), BST thin films show insulating character from room temperature down to 50K. It is quite clear from this plot that as deposited BST sample is in the topological transport regime. A crucial requirement for TI is an insulating bulk behavior i.e., the chemical potential should lie in the midst of the band gap, intersecting just the Dirac dispersion cones (and Rashba split bands discussed later). From the plot it can be inferred that our sample fulfills this condition. This is in stark contrast to other second generation TI samples such as BS & BT, which display metallic character. It displays clearly that at lower temperatures the bulk states start to localize while surface Dirac states remain delocalized and robust owing to spin momentum locking (Z_2 protection) and possession of a π Berry phase. Similar behavior has been observed in BTS and BST single crystals and other differently doped samples earlier but thin films of these ternary chalcogenides have rarely been studied^{19,20,26,28,30,31,35,42–47}. This type of character in BST thin films deposited by PLD has been observed for the first time. This behavior along with low temperature insulator to surface metallic transition ensures ordered occupancy of Se/Te in the quintuple layer unit, which is

consistent with the characteristic XRD peaks of ordered crystal structure of BST thin film. To confirm the insulating nature we had taken the data in both heating and cooling mode but the nature of R-T remained the same which is consistent with other reports. The novel features of the robust Dirac electrons are masked by the notorious trivial electrons of the bulk. The topological Transport regime ensures that this involvement of bulk and undesirable electrons in the transport measurements are kept to a minimum.

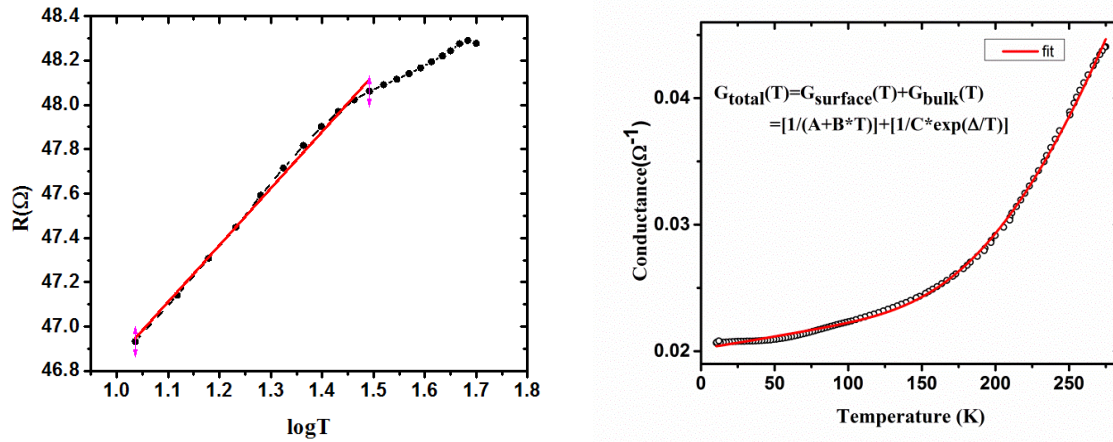


Fig. 3 (a) Plot of resistance vs. $\log(T)$ fitted to a linear curve from 50K down to 2K. From the decreasing trend it can be inferred that the sample exhibits WAL type behavior below 50K. (b) Conductance data fitted to a non-linear curve which includes both surface and bulk contribution to the conductance. A, B and C are constants and Δ represents the band gap.

Interesting features of the electron transport can be inferred from the temperature dependence of resistance, especially in the low temperature regime. The existence of WAL depends on the competition between the phase coherence of the electron wave function and the dephasing factors present in the system. Temperature plays a crucial role in this dephasing mechanism. With lowering temperature as the phonon contribution reduces in the system, a pronounced WAL type behavior can be seen in the R-T data. Therefore, temperature dependent WAL behavior below 50K can be represented by the following equation: $R(T) = R_1 - Q \log(T)$, where R_1 and Q are constants. This equation physically describes the WAL induced reduction in the resistance which is consistent with the recent theoretical reports⁴⁸. Thus, from the lowering of the resistance in the R-T profile we can infer the onset of WAL.

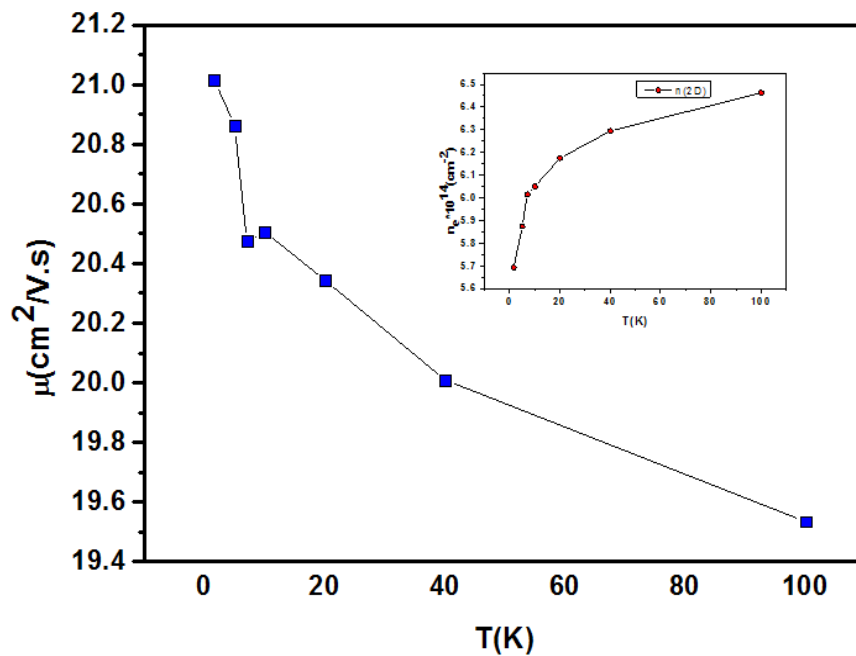


Fig. 4. Temperature dependence of mobility on is shown here. Mobility shows a decreasing trend with enhancement of temperature. Inset shows the 2D electron concentration increases with temperature as is expected (see text).

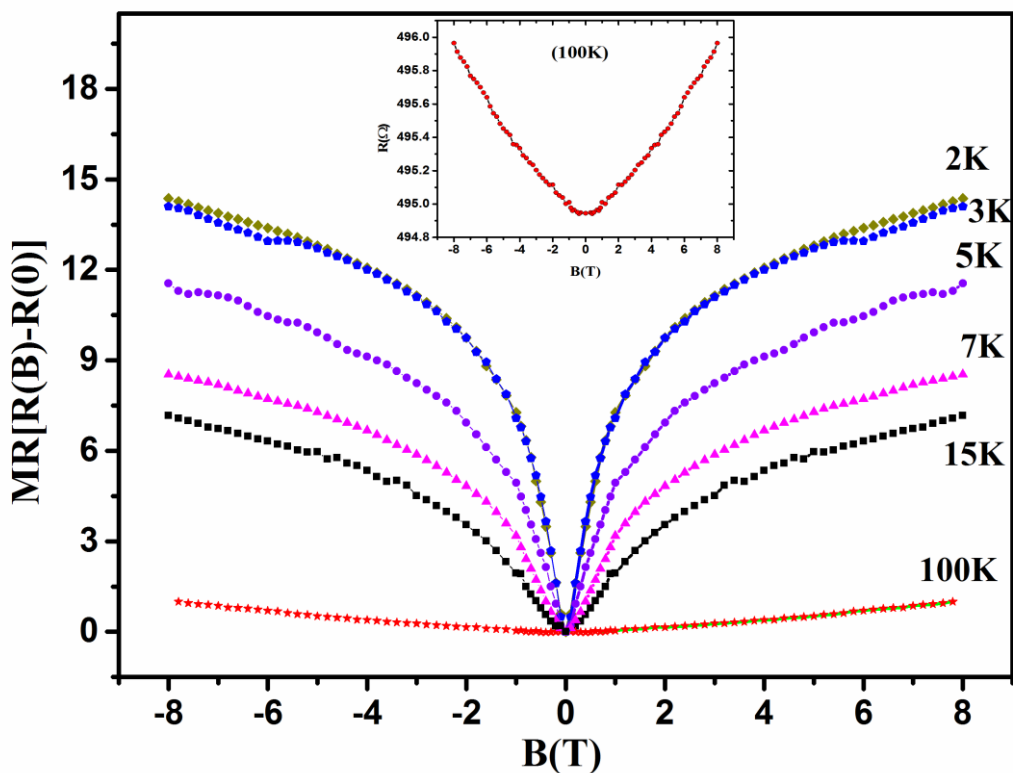


Fig. 5. Magnetoresistance (MR) at different temperatures. WAL is clearly comprehended from the above plot. The MR at 100K is shown in the inset which exhibits robust nature of surface Dirac states, but it is not characteristic WAL (sharp logarithmic dip in MR) rather it shows parabolic (B^2 dependence) MR followed by linear MR.

Observation of various quantum interference phenomena in TI has been one of the important tools to characterize the backscattering immune topological surface states. In high spin orbit coupled systems, having an odd number of Dirac cones the electron wave function gathers a “ π ” Berry phase as it circulates along a closed path on the isoenergetic Fermi circles in a Dirac cone. This results in destructive interference between two time reversed coherent loop/ paths of electron waves in a diffusive medium, effectively increasing the probability amplitude for forward scattering, while reduces the same for backscattering to almost zero¹⁴. These quantum interference phenomena manifest themselves in lowering the resistance or making positive correction to the conductivity (as shown in the R-T plot below 50K) at low temperatures. This phenomenon is known as weak antilocalization as opposed to its counterpart weak localization^{10,14,41,48–54}.

From the resistance vs. temperature plot we can surmise the existence of topological transport regime in the BST samples. Resistance of the thin films keeps on increasing as the temperature decreases till 50K and thereafter decreases with decreasing temperature. This feature can be attributed to the dominance of 2D Dirac surface state mediated WAL effect over electron-phonon interaction. The dominance of 2D WAL effect below certain temperature is an important observation in the bulk insulating TI's, where the contribution from bulk electrons and electron phonon (e-p) interaction die out. Below this critical temperature (50K), e-p interaction starts to weaken and bulk freezes out, Dirac fermions face lesser scattering and bulk coupling⁵⁵. As a result Dirac electrons surmount impurities/disorder more easily effectively increasing conductivity or making the system less dissipative, as we go down to lower temperatures. Therefore one can observe the WAL (intrinsic property of TI's) in the bulk insulating TI samples qualitatively by the nature of the R-T curve only. Therefore we have reached on important conclusion that 2D WAL in other higher bulk insulating TI candidates should start dominating at much higher temperatures, which is consistent with the previous reports on BTS, BSTS and some other intermediate intrinsic TI candidates^{13,22,28,32,33,35,42,56–58}. On the other hand this behavior further provides the proof for the weak e-p coupling between surface Dirac states and the bulk^{55,59,60}.

WAL in the TI thin films can also be probed by breaking the time reversal symmetry of the time reversed paths of Dirac electrons by the application of perpendicular magnetic field (B). It must be noted here that bare possession of π Berry phase by the surface Dirac states does not guarantee immunity to the disorder. Graphene possesses π Berry phase but exhibits WAL (positive MR) in a very short range of field and eventually localizes in the high field regime (negative MR). In contrast TI's exhibit a remarkable robustness to the applied field and does not

show any negative MR even up to the very high field regime (60T)⁶¹. This is attributed to the combined topological protection of the Dirac states (Z_2 protection along with π Berry phase) provided by their bulk band topology and single Dirac cone. Graphene consists of even number of Dirac cones on the surface Brillouin zone. Therefore it localizes due to inter-valley or intra-valley scattering, while in TI a single Dirac cone does not support these scattering processes due to absence of backscattering channels or valleys⁶²⁻⁶⁴. Therefore it is the topological distinction of the bulk band structure between TI's and graphene which separates both the materials in response towards application of field. It may be a possible reason for the non-saturating MR experimentally observed in TI thin films/devices.

A typical MR depicting WAL is shown in the Fig. 5 showing sharp increase in MR in the vicinity of zero field, a characteristic feature of WAL. From the temperature dependence of WAL it is clear it persists even at higher temperatures (100K), though reduced showing a remarkable robustness of the surface Dirac states towards electron-phonon interaction. This can only be attributed to the bulk insulating nature of these thin films. Low field nature of the 100K MR is the mixture of the classical ($MR \propto B^2$) and WAL induced MR. However, the classical MR dominates therefore it looks like parabolic in nature. In high field regime MR becomes almost linear and the possible reason for its origin is unknown and debatable. But some reports attribute linear response of MR to the surface states but at such a high temperature there can be sufficient electron-phonon and phonon-phonon interactions which may override the surface Dirac state contribution to conduction. But on the basis of some ARPES studies it has been found that surface Dirac states are very weakly coupled to the bulk phonon sea beneath, therefore we can attribute it to the mixed phase of MR from classical as well as quantum origin^{55,59}.

In presence of strong spin-orbit interaction, quantum correction to the conductivity in a two dimensional system can be described by Hikami, Larkin and Nagaoka (HLN) formula. This expression is applicable in the diffusive quantum transport regime with low mobility such as thin films deposited by PLD. The HLN equation can be written in the simplified form for the following condition: $\tau_{so} < \tau_e < \tau_\phi$, where τ_{so} , τ_e and τ_ϕ are the characteristic time scales corresponding to the spin-orbit scattering, elastic scattering and inelastic scattering of charge carriers. Conductance correction due to WAL is given as:

$$\delta G_{WAL}(B) \equiv G(B) - G(0) \cong \alpha \frac{e^2}{2\pi^2\hbar} \left[\Psi\left(\frac{1}{2} + \frac{B_\phi}{B}\right) - \ln\left(\frac{B_\phi}{B}\right) \right] \rightarrow (1)$$

Where Ψ is digamma function and $B_\phi = \hbar / 4el\phi^2$ is characteristic magnetic field corresponding to the coherence length l_ϕ . The value of coefficient α signifies effective number of coherent channels contributing to conduction.

Fitting of magneto-conductance by HLN equation in the low field regime at different temperatures is shown in the Fig. 6 (a) and the extracted parameters “ α ” and phase coherence

length are plotted as a function of temperature. The fitting parameters extracted from the fit are plotted in Fig. 6(b). In the bulk insulating and decoupled regime we have observed strong robustness of the conduction channel parameter “ α ” which hovers around “0.5”. This directs towards a single channel coherent transport. In such a situation it is very important to identify the dominant mechanism responsible for the robustness of α . The parameters which decide whether there is any surface to bulk coupling are τ_{sb} and τ_{ϕ} , where τ_{sb} is the effective surface to bulk scattering time and τ_{ϕ} is the phase coherence time. As long as τ_{sb} is greater than τ_{ϕ} , the bulk and surface serve as two independent channels since the carriers lose their coherence before they scatter into the bulk. But in the opposite scenario when the phase coherence time dominates over surface to bulk scattering time, the carriers maintain their coherence^{10,11,52,54}. This results in bulk and surface states behaving as if they possess an effective single phase coherent channel. In these films it is evident that the surface to bulk time τ_{sb} is very large compared to the phase breaking length τ_{ϕ} of surface Dirac fermions, i.e., $\tau_{\phi} \ll \tau_{sb}$, therefore there is no possibility for a surface to bulk coherent transport in such a situation. We can certainly say here that there is a decoupled transport and negligible contribution from the bulk^{10,22,54,57}.

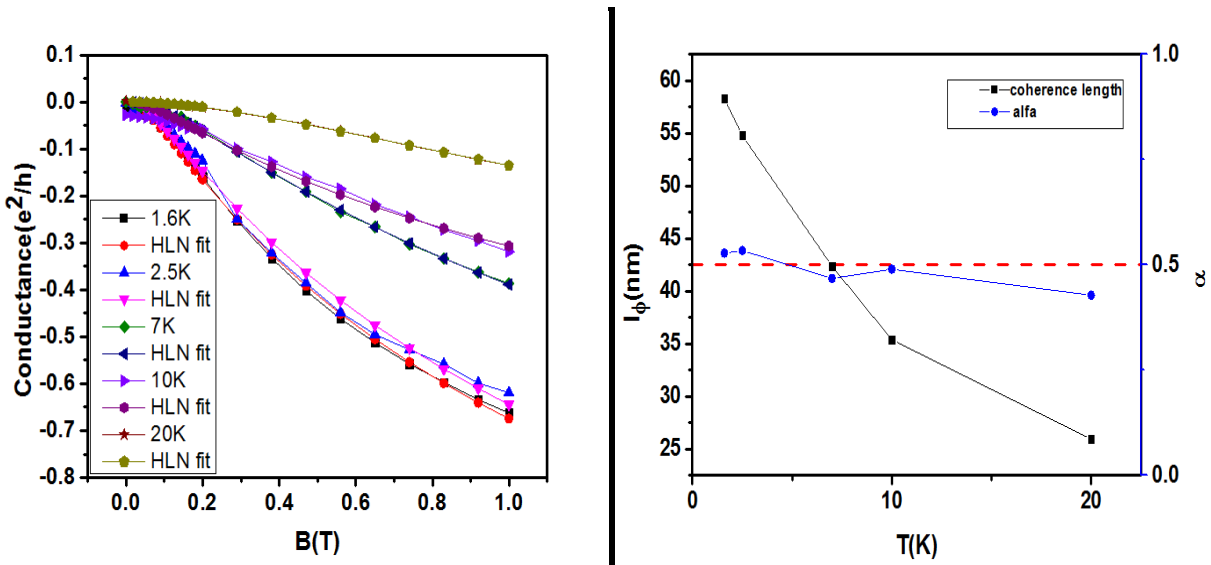


Fig. 6(a) HLN fit of conductance data at different temperatures. (b) Phase coherence length and α as a function of temperature.

From the magnetoconductance (MC/MR) analysis for these devices by 2D single channel Hikami Larkin Nagaoka Model we have observed that the coefficient “ α ” shows remarkable robustness in the temperature range 2.5K – 25K. The values of coefficient “ α ” obtained by fitting the change in $MC(\Delta G)$ vs. B data to the HLN model yielding around 0.5 signifying the presence of only one channel. Phase coherence length on the other hand decreases monotonically with increasing temperature which is justified. This is because, as the temperature of the system is increased phonons start creeping into the system. These phonons play a pivotal role in the dephasing mechanism and thus reduce the phase coherence length. The thickness of these devices are 300nm and 500nm, where there is no chance of coherent coupling to the bulk charge

carriers, since coherence length extracted at these temperatures are far too less (58nm) than the thickness of the devices. Moreover temperature dependent resistivity measurement suggests that no or negligible bulk state contribution exists at these temperatures providing further evidence of no surface to bulk coupling. The value of α signifies the number of conduction channels contributing to the conduction in a strongly spin orbit coupled two dimensional system. The value of α for TI thin films and devices extracted from the HLN model have been reported to vary between 0.3 – 1.5 and there is no general consensus among the various reported works. Thus a further modification in the exact model is required which describes topological behavior of TI transport^{2,40,65-68} and throw new light in this direction. Nevertheless HLN model captures almost all the features of the topological transport and the extracted parameters from the fitting of the MR have shown remarkable consistency with experimental observations depending on different physical conditions of TI sample.

Earlier studies based on the two channel conduction in TI thin films/ nano devices in ultrathin and thick limit have shown that the value of the coefficient α depends on various parameters such as gating voltage, compensation doping, intrinsic alloy solutions and thickness of the films/nano device at a particular temperature. There are reports indicating that the bulk states and quantum confined surface states in TI start localizing and at the same time when the Dirac surface states become more delocalized with decreasing temperature, owing to the reduced electron phonon interaction and spin momentum locking (π Berry phase). One can infer from the R – T plot this separation of the two regimes in the Fig. 2. Since bulk states are randomly oriented, on an average they do not exhibit WAL, while the trivial 2D surface states coexisting with surface Dirac fermions do not have topological protection and hence are not immune to the localization coming from disorder potential. These two mechanisms combined together may give rise to a weak localization correction component to the classical conductivity at low temperatures and hence an effective positive contribution to the total value “ α_T ” making it close to 0.5 as observed from the fitting to the HLN equation in Fig. 5(b).

The phase coherence length extracted from the fit does not show any improvement as is expected to be the case with the ternary tetradymides, high bulk insulating TI candidates exhibiting insulating nature in $\rho - T$ graph, underlying the fact that the Fermi level lies in the bulk gap (topological regime). One possible explanation for this type of behavior can be attributed to the coexistence of the two dimensional trivial electron gas (2DEG, Rashba split/band bending effect) on the surface participating in the 2D electron conduction along with the non- trivial Dirac fermions. This 2DEG could be localized completely at low temperatures by the disorder and grain boundaries present in PLD grown thin films. In our thin films there is a high possibility of band bending induced 2DEG owing to the exposure of external environment while making contacts before inserting samples in the measurement chamber.

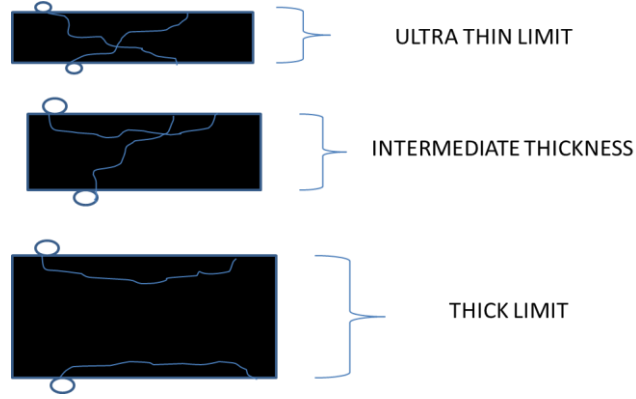


Fig.7 Coupled and decoupled transport of surface states.

We deposited thick films followed by annealing in the Argon environment for 2hrs in order to decouple the two surfaces and as a result we should have got the value of α around 1 – 1.15 as reported in some of the earlier works on thin films and single crystals. But the robustness of the value of α (0.5 – 0.6) with increasing temperature as extracted from the fitting of HLN equation has raised further questions. The only possible explanation for these values of α in decoupled regime can be competitive nature of WAL and WL originating from surface Dirac states and trivial quantum confined states respectively. For two surface states, WAL yields value of the coefficient α (which is negative and nearly ‘-1’ for capped TI thin films or unexposed to ambient atmosphere) and a positive value of α (say 0.4 - 0.3) coming from the localization of the nontrivial 2DEG and bulk impurity states, which comes in to play due to band bending/Rashba splitting and environmental exposure. Therefore, the resultant effect of these two phenomena results in the coefficient α to be -0.5. Quantitatively it can be expressed in the form of an equation.

$$\alpha_T = \alpha [\text{WAL} (-ve)] + \alpha [\text{WL} (+ve)] = 0.5 - 0.6$$

$$\alpha = f(\tau_\phi/\tau_{SB}) + f(\text{disorder or 2D quantum confined gas})$$

Surface reconstruction processes arising due to aging of sample in the external environment leading to downward band bending near the surface of TI thin films. These states quantum confined due to asymmetric potential can be shown as illustrated in the Fig.8 below schematically.

We need to reach almost ballistic regime ($k_{fe} \gg 1$ or $k_B T \tau / \hbar \gg 1$, mobility $\mu = 8000 - 20000 \text{ cm}^2/\text{Vs}$ or more) to observe the WAL in the 2D Rashba split quantum well states. One should have extremely low temperatures to observe WAL in these 2DEG systems (0.3 -10K) and at slightly high temperatures the WAL cusp in MR vanishes. These requirements to flip electron spin from random orientation by Rashba spin orbit interaction pose serious questions about the WAL behavior of 2DEG in heavily disordered systems⁶⁹ (mobility $\mu = 20 - 30 \text{ cm}^2/\text{Vs}$). This is

true in our case of polycrystalline thin films having larger grains which is evident from SEM data. The simultaneous observation of the clearly resolved beating pattern of SdH oscillations along with less sharp cusp of WAL (in the low field regime) in other 2D Rashba split systems allow us to conclude that in case of PLD deposited TI thin films 2DEG will rather exhibit some amount of localization due extremely low mobility (larger disorder).

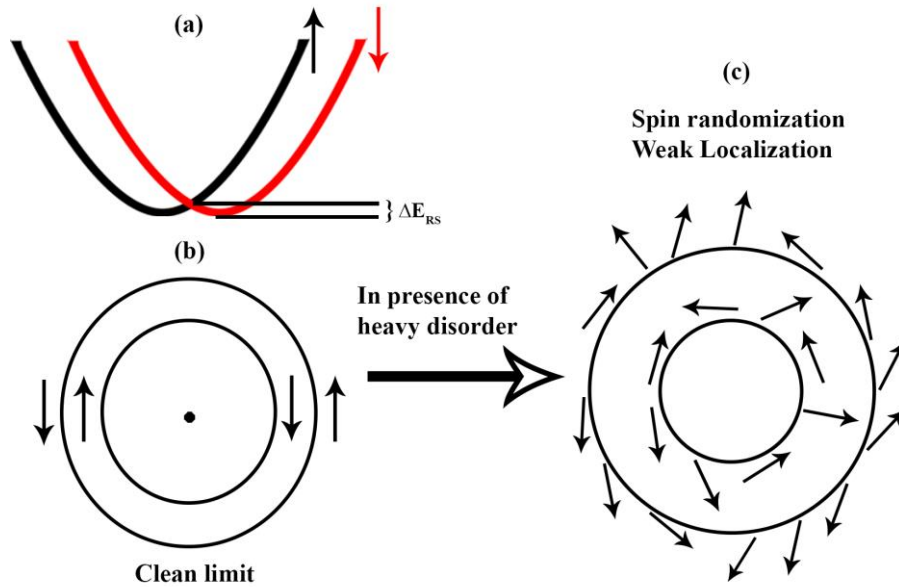


Fig. 8. (a) Rashba split bulk 2D sub-bands in TI due to formation of the quantum confined states at the surface. The arrows indicate spin direction of the electronic states. (b) Energy contour of these states and the channels for the inter-valley scattering in the clean limit (very high mobility). (c) Effect of the disorder on the spin orientation on these states exhibiting complete spin randomization, which suppresses WAL effectively. Note that the bulk conduction band and valence bands have not been shown in the figure. These states are just below the bulk conduction band.

WAL and SdH oscillations both show response to only perpendicular component of the magnetic field however there are some reports where SdH oscillations have shown contribution from the bulk as well. In case of sample surface degradation even by an hour exposure to ambient atmosphere, these quantum oscillations disappear but WAL on the other hand is remarkably robust even in samples exposed for many days. Hence we can claim that WAL is considerably reliable and a better tool to probe the TI surface states in comparison to SdH oscillations. Moreover to observe quantum oscillations in the samples of TI one needs to fulfill the condition; $\mu B \gg 1$ which require very high quality samples with high mobility and relatively high B field. On the other hand WAL is a low field phenomena and is observed in the range of 0- 1 Tesla.

WAL can be perceived in samples with very low carrier mobility (large disorder and in the presence of the grain boundaries, hence diffusive regime, i.e., $\mu B \ll 1$). PLD deposited films, are a lot more cost effective than single crystals.

Our argument is based on the premise that in PLD grown samples one cannot avoid the exposure from the external environment. Hence there is a surface degradation due to formation of the trivial 2DEG owing to the quantum confinement effects (downward band bending in our case because of n type carriers). This in turn results in enhancement of surface carrier density (as large as 40%). These trivial states are topologically unprotected and vulnerable to localization in the presence of disorder and grain boundaries. Their contribution to WAL is very feeble but by the same measure one cannot have quantum oscillations. Moreover the mobility and surface carrier density extracted by SdH analysis do not provide the Dirac fermionic nature and robustness of TI surface states. This in turn results in miscalculated value of mobility ' μ ' of the sample and erroneous value of surface Dirac carrier density which coexist with trivial 2DEG. These issues of correct Landau level indexing and extraction of Berry phase from the Landau level fan diagram have been addressed properly with their physical explanation by N.P. Ong and Y. Ando group^{13,24,35,47,65}.

In some reports,²⁷ it has been argued that quantum confined two dimensional electron states take part in WAL owing to the Rashba spin splitting, but these trivial 2DEG states may exhibit WAL only in low field regime (<100 mT) as compared to the WAL exhibited by topologically protected Dirac states (Tesla) which is three order of magnitude larger than the previous one. While 2DEG localizes in low field regime (<100 mT) showing a MR maximum and thereafter followed by negative MR exhibiting M like curve. But it has been observed in TI thin films that the sharp cusp like feature in MR lasts up to a high magnetic field range of several Tesla and followed by linear MR or quantum oscillations depending on the quality or strength of the applied external field. The magnitude of WAL cusp induced by topologically protected Dirac states is very large compared that of the trivial 2DEG so that it hardly affects the magnitude of WAL cusp (TI states). Therefore, contribution to the quantum correction to the conductivity from 2DEG is mainly from the localization channel of it. Moreover the Rashba splitting of quantum well states in TI thin films depends upon the time of the exposure and the type of the exposure which determine the nature of conduction, but the Rashba splitting energy in TI thin films exposed for a limited time has been found experimentally very weak. In such a case we could expect mainly weak localization contribution of 2DEG⁷⁰. Taskin et al¹² have clearly shown in their study on the formation of quantum well states and their effect on the surface conduction¹². In their study the value of transport coefficient " α " on the TI thin films of different thicknesses support our findings. Therefore, we can conclude from these arguments that the contribution of 2DEG to the transport coefficient " α " is only positive. Some recent transport studies on TI thin films with and without gating, support our findings and possible physical interpretation of extracted values of α in the passivated samples which protect the upper surface from degrading^{25,53}. In the decoupled transport from the two surfaces the value of α does not change and remains near to 1, signifying two channels^{10,25,26,54,57,71}.

Conclusion:

In this study our main focus was to optimize the BST samples in topological transport regime where bulk has negligible or very little significance in terms of contribution to transport as it is clearly manifested in the R – T plot. Secondly, we have prepared very thick films to decouple the two surface states with the bulk where condition $\tau_{\phi} / \tau_{sb} \ll 1$ is satisfied so that we could investigate the value of the transport channel coefficient “ α ” which in principle must be 1 for these samples. A coherent and comprehensive understanding has been given for the different values of the transport coefficient “ α ” based on experimental conditions and sample properties. It is remarkable feature that PLD grown thin films which are highly insulating in the bulk and thereby residing in the topological transport regime. PLD is a better deposition technique as compared to other synthesis techniques in terms of cost and time consumption to make a thin film. Annealing of the thin films in slightly elevated temperature makes the selenium atoms occupy ordered states between central layers of the Quintuple Layers. Thus annealing not only reduces the defects in the TI thin films but improves the surface morphology and smoothness, crystallinity and grain structure. In contrast to the restriction of observation of Quantum Oscillation only at very low temperature regime (due to thermal smearing of the cyclotron orbits) WAL is robust at higher temperatures exhibiting quantum coherence up to 100K, which makes it superior to SdH oscillations.

References

1. Hasan, M. & Kane, C. Colloquium: Topological insulators. *Rev. Mod. Phys.* **82**, 3045–3067 (2010).
2. Ando, Y. Topological Insulator Materials. *J. Phys. Soc. Japan* **82**, 102001 (2013).
3. Moore, J. E. The birth of topological insulators. *Nature* **464**, 194–198 (2010).
4. Qi, X.-L. *et al.* The quantum spin Hall effect and topological insulators. *Phys. Today* **63**, 55 (2010).
5. Kane, C. L. & Mele, E. J. Z_2 Topological Order and the Quantum Spin Hall Effect. *Phys. Rev. Lett.* **95**, 146802 (2005).
6. Fu, L. & Kane, C. Topological insulators with inversion symmetry. *Phys. Rev. B* **76**, 045302 (2007).
7. Kane, C. L. Condensed matter: An insulator with a twist. *Nat. Phys.* **4**, 348–349 (2008).
8. Bao, L. *et al.* Weak anti-localization and quantum oscillations of surface states in topological insulator $\text{Bi}_2\text{Se}_2\text{Te}$. *Sci. Rep.* **2**, 726 (2012).

9. Peng, H. *et al.* Aharonov-Bohm interference in topological insulator nanoribbons. *Nat. Mater.* **9**, 225–9 (2010).
10. Chen, J. *et al.* Gate-Voltage Control of Chemical Potential and Weak Antilocalization in Bi_2Se_3 . *Phys. Rev. Lett.* **105**, 1–4 (2010).
11. Steinberg, H., Gardner, D. R., Lee, Y. S. & Jarillo-Herrero, P. Surface State Transport and Ambipolar Electric Field Effect in Bi_2Se_3 Nanodevices. *Nano Lett.* 1–4 (2010). doi:10.1021/nl1032183
12. Taskin, A. A., Sasaki, S., Segawa, K. & Ando, Y. Manifestation of Topological Protection in Transport Properties of Epitaxial Bi_2Se_3 Thin Films. *Phys. Rev. Lett.* **109**, 066803 (2012).
13. Ren, Z., Taskin, A. A., Sasaki, S., Segawa, K. & Ando, Y. Large bulk resistivity and surface quantum oscillations in the topological insulator $\text{Bi}_2\text{Te}_2\text{Se}$. *Phys. Rev. B* **82**, 1–4 (2010).
14. Bergmann, G. Physical interpretation of weak localization: A time-of-flight experiment with conduction electrons. *Phys. Rev. B* **28**, 2914–2920 (1983).
15. Bergmann, G. WEAK LOCALIZATION IN THIN FILMS a time-of-flight experiment with conduction electrons. *Phys. Rep.* 1–58 (1913).
16. HJ, J. *Effects of Spin-Orbit Coupling on Quantum Transport. Physics*
17. Segev, M., Silberberg, Y. & Christodoulides, D. N. Anderson localization of light. *Nat. Photonics* **7**, 197–204 (2013).
18. Physics - Light Avoids Anderson Localization. at <<http://physics.aps.org/articles/v7/87>>
19. Qu, D.-X., Hor, Y. S., Xiong, J., Cava, R. J. & Ong, N. P. Quantum oscillations and hall anomaly of surface states in the topological insulator Bi_2Te_3 . *Science* **329**, 821–4 (2010).
20. Mi, J.-L. *et al.* Phase separation and bulk p-n transition in single crystals of $\text{Bi}_2\text{Te}_2\text{Se}$ topological insulator. *Adv. Mater.* **25**, 889 (2013).
21. Cao, H. *et al.* Quantized Hall Effect and Shubnikov–de Haas Oscillations in Highly Doped Bi_2Se_3 : Evidence for Layered Transport of Bulk Carriers. *Phys. Rev. Lett.* **108**, 216803 (2012).
22. Xu, Y. *et al.* Observation of topological surface state quantum Hall effect in an intrinsic three-dimensional topological insulator. *Nat. Phys.* **10**, 956–963 (2014).
23. Mellnik, a. R. *et al.* Spin-transfer torque generated by a topological insulator. *Nature* **511**, 449–451 (2014).

24. Xiong, J. *et al.* Quantum oscillations in a topological insulator Bi₂Te₂Se with large bulk resistivity (). *Phys. E Low-dimensional Syst. Nanostructures* **44**, 917–920 (2012).
25. Cao, H. *et al.* Controlling and distinguishing electronic transport of topological and trivial surface states in a topological insulator. (2014). at <<http://arxiv.org/abs/1409.3217>>
26. Hong, S. S., Cha, J. J., Kong, D. & Cui, Y. Ultra-low carrier concentration and surface-dominant transport in antimony-doped Bi₂Se₃ topological insulator nanoribbons. *Nature Communications* **3**, 757 (2012).
27. Lee, J., Lee, J.-H., Park, J., Kim, J. S. & Lee, H.-J. Evidence of Distributed Robust Surface Current Flow in 3D Topological Insulators. *Phys. Rev. X* **4**, 011039 (2014).
28. Ren, Z., Taskin, A. A., Sasaki, S., Segawa, K. & Ando, Y. Fermi level tuning and a large activation gap achieved in the topological insulator Bi₂Te₂Se by Sn doping. *Phys. Rev. B* **85**, 155301 (2012).
29. Miyamoto, K. *et al.* Topological Surface States with Persistent High Spin Polarization across the Dirac Point in Bi₂Te₂Se and Bi₂Se₂Te. *Phys. Rev. Lett.* **109**, 166802 (2012).
30. He, X. *et al.* Highly tunable electron transport in epitaxial topological insulator (Bi_{1-x}Sb_x)₂Te₃ thin films. *Appl. Phys. Lett.* **101**, 123111 (2012).
31. Gehring, P., Gao, B., Burghard, M. & Kern, K. Two-dimensional magnetotransport in Bi₂Te₂Se nanoplatelets. *Appl. Phys. Lett.* **101**, 023116 (2012).
32. Arakane, T. *et al.* Tunable Dirac cone in the topological insulator Bi_(2-x)Sb_(x)Te_(3-y)Se_(y). *Nat. Commun.* **3**, 636 (2012).
33. Pan, Y. *et al.* Low carrier concentration crystals of the topological insulator Bi_{2-x}Sb_xTe_{3-y}Se_y: a magnetotransport study. *New J. Phys.* **16**, 123035 (2014).
34. Ren, Z., Taskin, a., Sasaki, S., Segawa, K. & Ando, Y. Optimizing Bi_(2-x)Sb_(x)Te_(3-y)Se_(y) solid solutions to approach the intrinsic topological insulator regime. *Phys. Rev. B* **84**, 1–6 (2011).
35. Ren, Z., Taskin, A. A., Sasaki, S., Segawa, K. & Ando, Y. Observation of Dirac Holes and Electrons in a Topological Insulator. *Phys. Rev. B* **107**, 1–4 (2011).
36. Zhang, J. *et al.* Band structure engineering in (Bi_(1-x)Sb_(x))₂Te₃ ternary topological insulators. *Nat. Commun.* **2**, 574 (2011).
37. Nakayama, K. *et al.* Manipulation of Topological States and the Bulk Band Gap Using Natural Heterostructures of a Topological Insulator. *Phys. Rev. Lett.* **109**, 236804 (2012).

38. Shiomi, Y. *et al.* Spin-Electricity Conversion Induced by Spin Injection into Topological Insulators. *Phys. Rev. Lett.* **113**, 196601 (2014).
39. Bansal, N. *et al.* Epitaxial growth of topological insulator Bi₂Se₃ film on Si(111) with atomically sharp interface. *Thin Solid Films* **520**, 224–229 (2011).
40. Bansal, N., Kim, Y. S., Brahlek, M., Edrey, E. & Oh, S. Thickness-Independent Transport Channels in Topological Insulator Bi₂Se₃ Thin Films. *Phys. Rev. Lett.* **109**, 116804 (2012).
41. Kim, Y. S. *et al.* Thickness-dependent bulk properties and weak antilocalization effect in topological insulator Bi₂Se₃. *Phys. Rev. B* **84**, 1–5 (2011).
42. Jia, S. *et al.* Low-carrier-concentration crystals of the topological insulator Bi₂Te₂Se. *Phys. Rev. B* **84**, 235206 (2011).
43. Kong, D., Koski, K. J., Cha, J. J., Hong, S. S. & Cui, Y. Ambipolar field effect in Sb-doped Bi₂Se₃ nanoplates by solvothermal synthesis. *Nano Lett.* **13**, 632–6 (2013).
44. Lee, J., Park, J., Lee, J.-H., Kim, J. S. & Lee, H.-J. Gate-tuned differentiation of surface-conducting states in Bi_{1.5}Sb_{0.5}Te_{1.7}Se_{1.3} topological-insulator thin crystals. *Phys. Rev. B* **86**, 245321 (2012).
45. Mi, J.-L. *et al.* Phase separation and bulk p-n transition in single crystals of Bi₂Te₂Se topological insulator. *Adv. Mater.* **25**, 889–93 (2013).
46. Ren, Z., Taskin, A. A., Sasaki, S., Segawa, K. & Ando, Y. Large bulk resistivity and surface quantum oscillations in the topological insulator Bi₂Te₂Se. *Phys. Rev. B* **82**, 241306 (2010).
47. Xiong, J. *et al.* High-field Shubnikov–de Haas oscillations in the topological insulator Bi₂Te₂Se. *Phys. Rev. B* **86**, 045314 (2012).
48. Lu, H.-Z. & Shen, S.-Q. Finite-Temperature Conductivity and Magnetoconductivity of Topological Insulators. *Phys. Rev. Lett.* **112**, 146601 (2014).
49. Bao, L. *et al.* Weak anti-localization and quantum oscillations of surface states in topological insulator Bi₂Se₂Te. *Sci. Rep.* **2**, 726 (2012).
50. Lu, H.-Z. & Shen, S.-Q. Weak localization of bulk channels in topological insulator thin films. *Phys. Rev. B* **84**, 125138 (2011).
51. Liu, M. *et al.* Crossover between Weak Antilocalization and Weak Localization in a Magnetically Doped Topological Insulator. *Phys. Rev. Lett.* **108**, 036805 (2012).

52. Garate, I. & Glazman, L. Weak localization and antilocalization in topological insulator thin films with coherent bulk-surface coupling. *Phys. Rev. B* **86**, 035422 (2012).
53. Lang, M. *et al.* Revelation of topological surface states in Bi₂Se₃ thin films by in situ Al passivation. *ACS Nano* **6**, 295–302 (2012).
54. Kim, D., Syers, P., Butch, N. P., Paglione, J. & Fuhrer, M. S. Coherent topological transport on the surface of Bi₂Se₃. *Nat. Commun.* **4**, 1–5 (2013).
55. Pan, Z.-H. *et al.* Measurement of an Exceptionally Weak Electron-Phonon Coupling on the Surface of the Topological Insulator Bi₂Se₃ Using Angle-Resolved Photoemission Spectroscopy. *Phys. Rev. Lett.* **108**, 187001 (2012).
56. Barreto, L. *et al.* Surface-dominated transport on a bulk topological insulator. *Nano Lett.* **14**, 3755–60 (2014).
57. Kong, D. *et al.* Ambipolar field effect in the ternary topological insulator (Bi_xSb_{1-x})₂Te₃ by composition tuning. *Nature Nanotechnology* **6**, 705–709 (2011).
58. Xiong, J., Khoo, Y., Jia, S., Cava, R. J. & Ong, N. P. Tuning the quantum oscillations of surface Dirac electrons in the topological insulator Bi₂Te₂Se by liquid gating. *Phys. Rev. B* **88**, 035128 (2013).
59. Sobota, J. A. *et al.* Distinguishing Bulk and Surface Electron-Phonon Coupling in the Topological Insulator Bi₂Se₃ Using Time-Resolved Photoemission Spectroscopy. *Phys. Rev. Lett.* **113**, 157401 (2014).
60. Wang, Y. H. *et al.* Measurement of Intrinsic Dirac Fermion Cooling on the Surface of the Topological Insulator Bi₂Se₃ Using Time-Resolved and Angle-Resolved Photoemission Spectroscopy. *Phys. Rev. Lett.* **109**, 127401 (2012).
61. Zhang, S. X. *et al.* Magneto-resistance up to 60 Tesla in topological insulator Bi₂Te₃ thin films. *Appl. Phys. Lett.* **101**, 202403 (2012).
62. Wu, X., Li, X., Song, Z., Berger, C. & de Heer, W. A. Weak Antilocalization in Epitaxial Graphene: Evidence for Chiral Electrons. *Phys. Rev. Lett.* **98**, 136801 (2007).
63. Gorbachev, R. V., Tikhonenko, F. V., Mayorov, A. S., Horsell, D. W. & Savchenko, A. K. Weak Localization in Bilayer Graphene. *Phys. Rev. Lett.* **98**, 176805 (2007).
64. Tikhonenko, F. V., Kozikov, A. A., Savchenko, A. K. & Gorbachev, R. V. Transition between Electron Localization and Antilocalization in Graphene. *Phys. Rev. Lett.* **103**, 226801 (2009).
65. Taskin, A. A. & Ando, Y. Berry phase of nonideal Dirac fermions in topological insulators. *Phys. Rev. B* **84**, 035301 (2011).

66. Steinberg, H., Laloë, J.-B., Fatemi, V., Moodera, J. S. & Jarillo-Herrero, P. Electrically tunable surface-to-bulk coherent coupling in topological insulator thin films. *Phys. Rev. B* **84**, 233101 (2011).
67. Bahramy, M. S. *et al.* Emergent quantum confinement at topological insulator surfaces. *Nat. Commun.* **3**, 1159 (2012).
68. Cha, J. J. *et al.* Weak antilocalization in Bi₂(Se(x)Te(1-x))₃ nanoribbons and nanoplates. *Nano Lett.* **12**, 1107–11 (2012).
69. Miller, J. B. *et al.* Gate-Controlled Spin-Orbit Quantum Interference Effects in Lateral Transport. *Phys. Rev. Lett.* **90**, 076807 (2003).
70. Lang, M. *et al.* Competing weak localization and weak antilocalization in ultrathin topological insulators. *Nano Lett.* **13**, 48–53 (2013).
71. Jauregui, L. A., Pettes, M. T., Rokhinson, L. P., Shi, L. & Chen, Y. P. Gate Tunable Relativistic Mass and Berry's phase in Topological Insulator Nanoribbon Field Effect Devices. 22 (2014). at <<http://arxiv.org/abs/1402.2659>>
72. 70. It should be noted here that in ref.26 thickness of the thin films is in coupled regime ($l\phi \geq t$, where t is thickness of the thin film) and nearly metallic in nature effectively making coherently coupled single channel transport at given thicknesses. In decouples regime we believe, such passivated thin films will result $\alpha = 1$. See also supplementary information of ref.54,71 and 12.